Strojniški vestnik - Journal of Mechanical Engineering 70(2024)3-4, 141-158
DOI:10.5545/sv-jme.2023.691
Original Scientific Paper
Received for review: 2023-06-14
Received revised form: 2023-11-05
Accepted for publication: 2023-11-27

Transient Flow Characteristics of a Pressure Differential Valve with Different Valve Spool Damping Orifice Structures

Xu Zhang
Fluid Machinery Engineering Technology Research Centre of Jiangsu University, China

Lubrication system failure is a significant cause of in-flight shutdown incidents in aviation engines. The pressure differential valve, an essential component of a certain type of aviation engine lubrication system, is responsible for controlling the flow rate and pressure of the lubricating oil. Comprehending the transient flow characteristics of the pressure differential valve is of paramount importance for the secure operation of lubrication systems. This paper establishes a transient flow model of a pressure differential valve based on a transient computational fluid dynamics (CFD) method, and the experimental validation demonstrates the effectiveness of the computational model. The internal flow characteristics of the differential pressure valve at different stages during the opening process were studied. Additionally, four transient lubricating oil flow models with different valve spool damping orifice were established to analyse the impact of damping orifice structure on valve spool movement characteristics, pressure control characteristics, and flow field distribution. The results indicate that when the diameter of the valve spool damping orifice increases from 0.3 mm to 1.0 mm, the valve spool displacement and fluid force increase by 88 % and 20 %, respectively. Meanwhile, the peak valve spool velocity, peak oil supply pressure, and steady-state value decreased by 15 %, 29 %, and 34 %, respectively. As the length of the valve spool damping orifice increases from 0.894 mm to 4.0 mm, the growth rate of valve spool displacement and fluid force gradually decreases, with the peak valve spool velocity decreasing by 7 %. This study has potential significance for the structural optimization and application of pressure differential valve in lubrication systems.

Keywords: aviation engine lubrication system, pressure differential valve, flow impact, transient flow, valve spool damping orifice

Highlights

- *The spring force and fluid force jointly affect the pressure-regulating characteristics of the pressure differential valves.*
- *When the valve spool damping orifice structure is Φ0.3×0.894, the pressure regulation performance is poor.*
- *Increasing the diameter of the damping orifice can effectively reduce the maximum oil supply pressure, increasing the length of the damping hole has little effect on the oil supply pressure.*
- *The damping orifice structure of the pressure differential valve has little effect on the start time of the valve spool.*

0 INTRODUCTION

As one of the key systems of aviation engines, the lubrication system has a significant impact on the safe operation of the engine due to its lubrication performance [1]. According to relevant statistical data, in the engine shutdown accidents of the Chinese Air Force in 1985, lubrication system failures accounted for as much as 43 % of such cases. Similarly, a certain type of aviation engine in the US Air Force experienced 90 aviation accidents in just one year, of which 28 % were due to lubrication system failures [2]. The lubrication system undertakes the task of providing sufficient lubricating oil for aviation engines, as well as lubricating and cooling the supporting bearings and transmission components, reducing friction and temperature between each component, alleviating the ultra-high heat generated by mechanical friction, and preventing important parts from clogging and corrosion during operation [3] to [5]. Currently, the lubrication oil supply subsystem of foreign military aviation engines (such as the F110 military engine from GE in the United States and the АЛ-31Ф engine from Russia) commonly uses a fixed pressure valve to control the lubrication system flow. However, a certain type of domestically developed fighter jet in China uses a pressure differential valve to control the circulation of the lubrication oil supply system [6]. Compared with the traditional fixed-pressure oil supply method, the pressure differential valve pays more attention to the stability of the oil supply under high-speed and high-pressure conditions, making the aircraft more adaptable and providing certain excellent guarantees for the safe operation of aviation engines [7] and [8]. However, at present, there is relatively limited theoretical and experimental research data on this valve, especially regarding the transient flow of high-pressure lubricating oil inside the pressure differential valve, and relevant data is relatively scarce. Therefore, an in-depth exploration of the pressure-regulating valve has significant practical significance.

With the development of the industrial field, especially in the aerospace industry, the requirements for the pressure-regulating characteristics of valves are gradually increasing. Therefore, research on the

*Corr. Author's Address: Fluid Machinery Engineering Technology Research Centre of Jiangsu University, China, 18993458481@163.com

transient opening process of pressure differential valves is becoming increasingly important. Lai et al. [9] used unsteady computational fluid dynamics (CFD) methods to investigate the transient characteristics and internal flow distribution of dual disc check valve, and verified the reliability of CFD results through experiments, providing an approximate value of disc rotation characteristics. Afshari et al. [10] conducted research on some key parameters that have a significant impact on the dynamic response of direct-acting hydraulic pressure-reducing valves using bond graph simulation technology and proposed an analytical solution applicable to nonlinear complex systems with multiple energy domain interactions. Cui et al. [11] utilized the user-defined function UDF technology and mobile grid technology to conduct unsteady research on the opening and closing process of a ball valve. The results showed that due to the fluid lag and changes in the relative opening, there were significant differences in the transient performance and flow field of the ball valve during the opening and closing process. Sibilla et al. [12] studied the internal flow characteristics of the check valve based on the transient CFD model and dynamic mesh technology. In addition, the influencing factors of flow characteristics during valve opening and closing are also studied. Beune et al. [13] designed CFD software to analyse the opening characteristics of high-pressure safety valves, and studied the relationship between disk lift, flow force and mass flow rate versus time.

Chattopadhyay et al. [14] studied the internal flow structure of the spool-type pressure regulating valve at different openings and different pressure drops and found that the standard $k-\varepsilon$ turbulence model can predict higher levels of turbulent kinetic energy. In addition, it was found that the two-dimensional axisymmetric formula can capture the total flow parameters well. Han et al. [15] studied the variation of flow rate and pressure difference with time during the opening and closing process of the ball valve by using dynamic mesh technology and variable inlet and outlet boundary conditions. Saha et al. [16] studied the transient flow characteristics inside the shut-off valve and found that the higher the friction coefficient between the valve spool and the valve body, the faster the stability of the spool. Ray [17] established a nonlinear dynamic model of the relief valve and studied its transient response. It was found that the valve opening time was linearly related to the dimensionless parameters given by the ratio of the orifice length to its radius. Dasgupta [18] studied the dynamic characteristics of the pilot relief valve based on bond graph technique, and determined some key design parameters that have a significant impact on the dynamic response of the valve through simulation research. Zhang et al. [19] studied the full transient opening dynamic characteristics of the 3D power-operated pressure relief valve and obtained the pressure field and velocity field, including small-scale flow characteristics. Sun et al. [20] analysed the transient flow mechanism during the opening of the integrated valve and the variation of the transient characteristic parameters of the valve-induced pressure with the operating temperature, the initial flow rate of the fluid and the opening time of the valve. Yang et al. [21] studied the opening and closing process of a steam pressure relief valve in a nuclear power plant by using CFD technology combining the domain decomposition method (DDM) and the grid pre-deformation method (GPM) methods and found that reducing spring stiffness can effectively reduce the reseating pressure.

In addition, in order to adapt to the requirements of various industries and improve the working efficiency and voltage regulation characteristics of the valve, much research has been done on its structural design. Abdallah et al. [22] studied the relationship between different inlet pressures and pressure oscillation and proposed four solutions to reduce the pressure oscillation of the deflection jet servo valve by structural optimization. Zang et al. [23] studied the influence of different inlet diameters on the dynamic characteristics of the pilot valve by using dynamic mesh technology. The results show that increasing the inlet diameter can significantly shorten the opening time of the valve, but also increase the fluid force and velocity of the valve spool during the opening process. Liu et al. [24] used AMESim to study the effects of spring stiffness and preload on the dynamic characteristics of a three-way proportional reducing valve, and the experimental results were consistent with the simulation results. In addition, it was found that using closed-loop control of valve lift can effectively improve the dynamic characteristics. Combined with numerical calculation and experimental verification, Simic et al. [25] studied all geometric parameters of the valve to optimize the valve geometry. The results show that the axial component of the flow force can be significantly reduced, and the dynamic characteristics of the valve can be improved only by modifying the geometry of the spool and the valve shell. Liu et al. [26] proposed a structure for compensating the hydrodynamic force of the cartridge cone valve, and studied several parameters that may affect the hydrodynamic characteristics. The results show that the hydrodynamic compensation effect

of the valve core increases with the increase of the opening degree under the optimal size. Ye et al. [27] established a CFD model of a high-pressure hydrogen needle valve and studied the influence of valve spool shape on the performance and flow characteristics of the valve. The results show that changing the shape of the valve spool to make it have a larger flow area at a small opening can make the high-pressure hydrogen valve have a better flow field distribution. In addition, Ye et al. [28] studied the influence of spool head angle on spool motion performance and flow field characteristics. The results show that the acceleration, velocity, and kinetic energy of the valve spool increase with the increase of the valve spool head angle, which enhances the impact effect of the valve spool. Yang et al. [29] established the simulation model of the relief valve and analysed the influence of valve seat flow path diameter and valve seat chamfering depth on valve flow field performance. The results show that increasing the diameter of the flow path helps to suppress the negative pressure, and increasing the chamfering depth of the valve seat can reduce the flow rate and the maximum negative pressure of the throat. Han et al. [30] has proposed a novel fast-response water hydraulic proportional valve and developed an accurate nonlinear mathematical model to simulate its dynamic performance. Experimental results have demonstrated the valve's excellent static and dynamic control capabilities. Karanović et al. [31] conducted experimental research using a mechanically actuated 4/2 control valve to investigate the wear intensity of working elements under different levels of oil contamination by solid particles. Additionally, by measuring the pressure drop values during fluid flow through the valve, it was observed that oils with the lowest cleanliness level exhibited greater variability in the measured values. These results provide insights into the impact of working fluid cleanliness on potential defects and failures within hydraulic system components, thereby contributing to a better understanding of their reliability and durability.

The references show that there is less research on pressure differential valve under high-pressure lubricating oil flow conditions. Therefore, the main purpose of this paper is to explore the transient characteristics of pressure differential valve under the impact of high-pressure lubricating oil, quantify the movement and force of the valve spool, and summarize the influence of different valve spool damping orifice structures on the pressure regulating characteristics of the valve. It provides research accumulation for the structural optimization and application of pressure differential valve in aero-engine lubrication system. The specific research process is as follows. Firstly, the transient flow field characteristics during the opening process of the pressure differential valve are studied. Secondly, the variation of displacement, velocity, fluid force, oil supply pressure and other parameters during the transient opening process of pressure differential valve under different valve spool damping orifice structures are analysed. Finally, the movement law and pressure regulation characteristics of the valve spool under the impact of high-pressure lubricating oil are quantitatively analysed.

1 TRANSIENT CFD MODEL PRESSURE DIFFERENTIAL VALVE

1.1 Geometry of Pressure Differential Valve and 3D Model

Fig. 1 is a functional diagram of pressure differential valve. The valve spool can move back and forth under the combined action of spring force, inlet pressure, oil supply pressure, middle cavity pressure, hydraulic force, etc., thereby changing the opening size of the overflow orifice and ensuring that the pressure difference before and after each lubricating nozzle is stable within the specified range. The excess lubricating oil at the outlet of the lubricating oil pump is returned to the oil tank through the overflow pipeline to adjust the oil supply of the lubrication system.

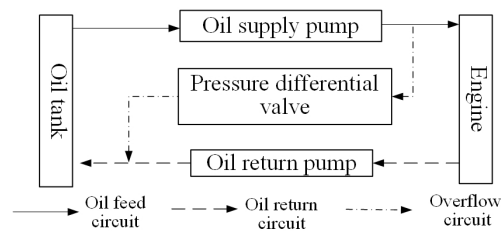

Fig. 1. *Functional diagram of pressure differential valve*

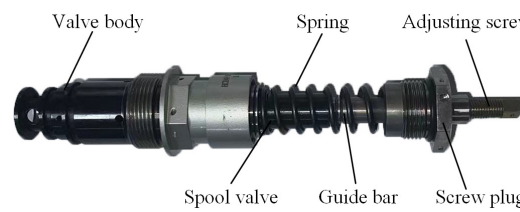

Fig. 2. *Physical diagram of pressure differential valve*

Fig. 2 is a physical diagram of pressure differential valve, which is widely applied in the lubrication system of aviation engines. It is installed on the lubrication oil pump to control the oil supply and pressure of the lubrication system and has a

certain impact on the stability of the aviation engine lubrication system.

Fig. 3 shows a 3D half section view of pressure differential valve, the valve is composed of a valve enclosure, valve body, valve spool, guide rod, screw plug, adjusting screw, and spring. Lubricating oil flows into the valve through the left inlet port. From the inlet of the valve, the overflow orifices, oil supply pressure inlet orifices, and middle cavity pressure orifices are located in succession from left to right. There are four orifices for each passage. Among them, the diameters are 6 mm, 2 mm, and 3 mm respectively, and the four orifices in each part are evenly distributed in the circumferential direction. The maximum outer diameter of the inner chamber of the valve is 22 mm, and the valve spool inside is a hollow structure with a damping orifice. After measurement, the mass of the valve spool is 50 g, the maximum stroke is 9 mm, the spring stiffness coefficient is 4900 N/m, and the preload is 69.8 N. There are two valve limits on the valve body to limit the displacement of the valve spool. When the pressure differential valve is opened, the valve spool stops moving when the end face of the valve spool contacts with the limit surface.

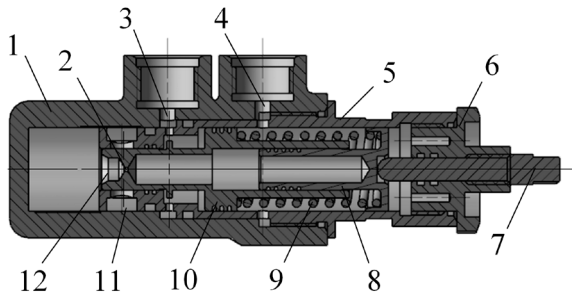

Fig. 3. *Half sectional view of pressure differential valve; 1 valve enclosure, 2 damping orifice, 3 oil supply pressure inlet, 4 medium cavity pressure inlet, 5 valve body, 6 screw plug, 7 adjusting screw, 8 guide rod, 9 spring, 10 valve spool, 11 overflow orifice, 12 valve inlet*

The internal structure of the valve spool is a cavity with a damping orifice, the diameter of which is 1mm and the length is 0.894 mm. The valve can set the initial opening pressure by adjusting the preload of the spring through the adjusting screw. At this time, due to the compression of the spring, the valve spool is located at a displacement of 0 under the action of the spring force, and the overflow orifices are closed. After the lubrication system starts to work, the lubricating oil enters the valve and the oil supply chamber under the action of the lubrication oil pump. The valve spool begins to move under the combined effect of the inlet pressure, oil supply pressure, middle cavity pressure, spring force, valve spool internal cavity pressure, hydraulic force, etc. As the displacement increases, the overflow orifices are opened, thereby regulating the average oil supply pressure and fluctuation amplitude.

1.2 Numerical Theory of Valve Spool Dynamic Balance

Fig. 4 is the simplified physical model of pressure differential valve. The pressure differential valve controls the oil supply pressure through the movement state of the valve spool; displacement determines the valve opening size. In the process of pressure regulation, the force of the valve spool in the lubricating oil is complex and changeable. In order to correctly build a simulation model to understand the transient flow characteristics of the high-pressure lubricating oil inside the pressure differential valve, it is particularly important to analyse the force of the valve spool. Many non-linear factors exist in the mathematical model for valve dynamic characteristics, such as hydraulic power, pipeline dynamic transmission characteristics, etc. At the same time, the work process has a number of interfering factors. Hence, factors like hydraulic pressure, viscous friction force, the spring force, the steady-state hydrodynamic force, and the transient hydrodynamic force must be fully considered in the development of the mathematical model.

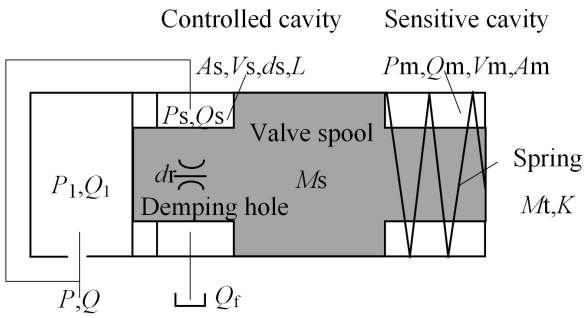

Fig. 4. *Physical model of pressure differential valve*

Valve spool force balance equation, Eq. (1):

$$P_1A_1 - P_2A_2 + P_sA_s - P_mA_m + F_{stf} + F_{trf} - K(X_{s0} + X_s) \mp F_f = (M_s + \tfrac{1}{3}M_t)\frac{d^2X_s}{dt^2} + B_s\frac{dX_s}{dt}, \quad (1)$$

where $A_1 = A_2$, A_1 is the force area of the inlet end of the valve, A_2 is the force area of the rear cavity of the damping orifice, A_s is the force area of the oil supply cavity, and A_m is the force area of the middle cavity. P_1 is the inlet pressure of pressure differential valve, and P_2 is the cavity pressure behind damping orifice.

P_s is the pressure of the oil supply cavity, and P_m is the pressure of the middle cavity. M_s is the mass of the valve spool, M_t is the mass of the spring, K is spring stiffness, X_{s0} is the pre-compression of the spring, and X_s is the displacement of the valve spool.

Valve spool motion damping coefficient B_s:

$$B_s = \frac{\pi \eta l d}{(D-d)}, \tag{2}$$

where D and d are the diameter of the valve cavity and the diameter of the valve spool respectively, and l is the damping length.

F_{stf} and F_{trf} are steady-state hydrodynamic force and transient hydrodynamic force, respectively. The expressions are as follows:

$$F_{stf} = -K_s X_s P_s, \tag{3}$$

$$F_{trf} = K_L \frac{dX_s}{dt}, \tag{4}$$

where K_s is the steady-state hydrodynamic coefficient, and K_L is the transient hydrodynamic viscous damping coefficient.

1.3 Control Equations

Numerical solutions in CFD utilize fundamental equations including the continuity equation, momentum equation, and energy equation. In this study, the CFD simulation of pressure differential valve does not consider energy transfer; therefore, the energy equation is not considered. Additionally, CFD also includes component mass conservation equations for various chemical components and equations of state for gases with density variations. Different equations need to be introduced to describe different problems. The fundamental equations of fluid mechanics are always closed, and the corresponding numerical solutions are obtained by discretizing these equation groups.

The continuity equation, also known as the mass conservation equation, states that any fluid flow must satisfy the law of mass conservation. The continuity equation can be expressed as:

$$\frac{\partial \rho}{\partial t} + div(\rho \vec{u}) = 0\,. \tag{5}$$

Written in the form of divergence, it can be expressed as:

$$\frac{\partial \rho}{\partial t} + \frac{\partial(\rho u)}{\partial x} + \frac{\partial(\rho v)}{\partial y} + \frac{\partial(\rho w)}{\partial z} = 0, \tag{6}$$

where ρ represents the density of the fluid; u, v and w represent the velocity components of the fluid element in the X, Y, and Z directions; t represents time.

Momentum equation:

To solve any fluid flow problem, it is necessary to satisfy the momentum equation, which is a fundamental equation. For incompressible Newtonian fluids, the conservation equation of momentum for a viscous, incompressible flow can be represented by the following form of the Navier-Stokes (N-S) equation:

$$\begin{aligned}
&\rho\left(\frac{\partial u}{\partial t} + u\frac{\partial u}{\partial x} + v\frac{\partial u}{\partial y} + w\frac{\partial u}{\partial z}\right) = \\
&\rho F_x - \frac{\partial p}{\partial x} + \mu\left(\frac{\partial^2 u}{\partial x^2} + \frac{\partial^2 u}{\partial y^2} + \frac{\partial^2 u}{\partial z^2}\right), \\
&\rho\left(\frac{\partial v}{\partial t} + u\frac{\partial v}{\partial x} + v\frac{\partial v}{\partial y} + w\frac{\partial v}{\partial z}\right) \\
&= \rho F_y - \frac{\partial p}{\partial y} + \mu\left(\frac{\partial^2 v}{\partial x^2} + \frac{\partial^2 v}{\partial y^2} + \frac{\partial^2 v}{\partial z^2}\right), \\
&\rho\left(\frac{\partial w}{\partial t} + u\frac{\partial w}{\partial x} + v\frac{\partial w}{\partial y} + w\frac{\partial w}{\partial z}\right) \\
&= \rho F_z - \frac{\partial p}{\partial z} + \mu\left(\frac{\partial^2 w}{\partial x^2} + \frac{\partial^2 w}{\partial y^2} + \frac{\partial^2 w}{\partial z^2}\right),
\end{aligned} \tag{7}$$

where ρ represents the density of the fluid; μ represents the dynamic viscosity of the fluid; u, v and w represent the velocity components of the fluid element in the X, Y, and Z directions, respectively; p represents the pressure on the fluid element; t represents time; F_x, F_y, and F_z represent the components of external forces in the X, Y, and Z directions.

The Navier-Stokes equations consist of 3 fractional equations, plus the continuity equation, resulting in a total of 4 equations with 4 unknowns: u, v, w and p. The equation group is closed, and with proper initial and boundary conditions, the equations can be solved.

1.4 Computational Fluid Domain and Grid Independence Verification

In order to analyse the real transient flow inside the valve, the lubricating oil pump and pressure differential valve are connected through the pipeline for joint simulation. The fluid domain is shown in Fig. 5, and the fluid domain of the lubricating oil pump and pressure differential valve is shown in Fig. 6. In the actual lubrication process, the lubricating oil is sprayed to each lubrication point through the nozzle,

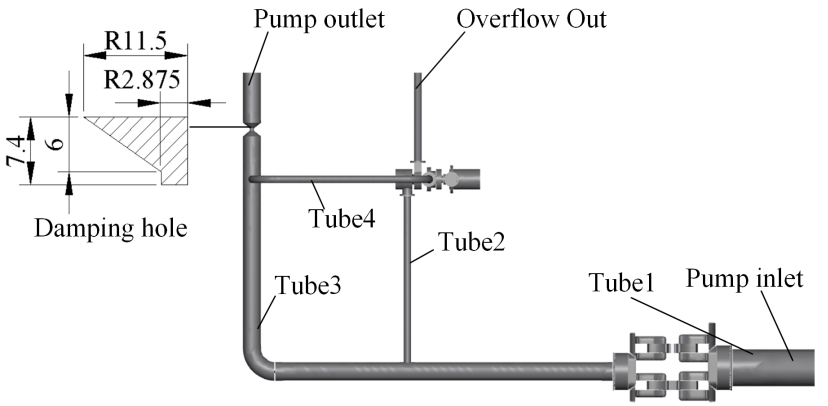

Fig. 5. *Schematic diagram of pump and valve fluid domain*

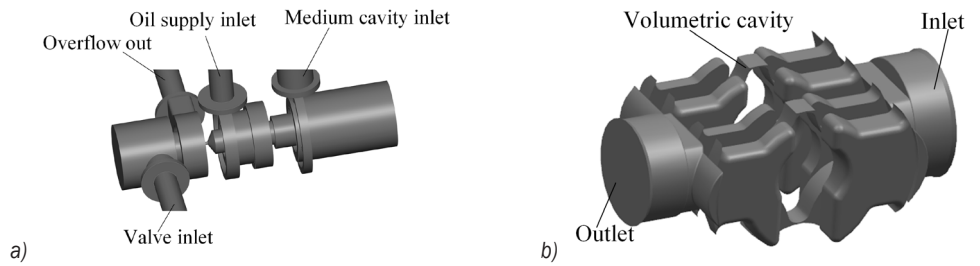

Fig. 6. *Computational fluid domain of main components; a) pressure differential valve, and b) lubricating oil pump*

and the damping orifice is designed to make the simulation closer to the test. The size of each part of the pipeline is shown in Table 1.

Table 1. *Pipeline parameters*

Name	Diameter [mm]	Length [mm]
Tube1	40	400
Tube2	8	180
Tube3	20	650
Tube4	12	280

Table 2. *Rotation centre coordinates*

Coordinate	rotor pair 1		rotor pair 2	
	internal rotor	external rotor	internal rotor	external rotor
X [mm]	294	294	294	294
Y [mm]	0	–4.5	0	–4.5
Z [mm]	207	207	247	247

Pumplinx software has a dedicated meshing template for internal gear pumps and a slide valve meshing template. First, the rotor template mesher module is used to divide the intermeshing region of the lubricating oil pump rotor. The internal rotor has 4 teeth, and the external rotor has 5 teeth. The rotation axis is the Z axis. The rotation centre is set as shown in Table 2, and the rotor mesh size is set to a high-quality mesh.

When the valve spool moves, pressure differential valve has a volume chamber that is stretched and compressed. Therefore, the valve template mesh module is used to divide the corresponding fluid domain, and the moving surface, cylindrical surface and end surface of the volume cavity are set. The direction of motion is X-axis, the minimum gap is 0.1 mm, and the maximum stroke is 9 mm. Because the valve spool is a moving part, the valve spool is also meshed by valve template mesh module. The rest parts, such as connecting pipelines and lubricating oil pump inlet and outlet, are divided into grids by general mesher module.

Table 3. *Number of grids*

Scheme	Number of grids [×10⁴]	Pump outlet flow rate [m³/h]	Overflow rate [m³/h]
a	39	2.77	1.54
b	70	2.57	1.41
c	138	2.55	1.40
d	263	2.54	1.40

The number of grids is shown in Table 3. The pump outlet flow rate and valve overflow flow rate under each scheme are shown in Fig 7. Comparison

shows that scheme a has a significant difference from the other three schemes, with a much smaller number of meshes, which seriously affects the calculation results. Considering comprehensively, scheme b is finally selected as the number of grids calculated in this paper. The grids of pressure differential valve and lubricating oil pump are shown in Fig. 8.

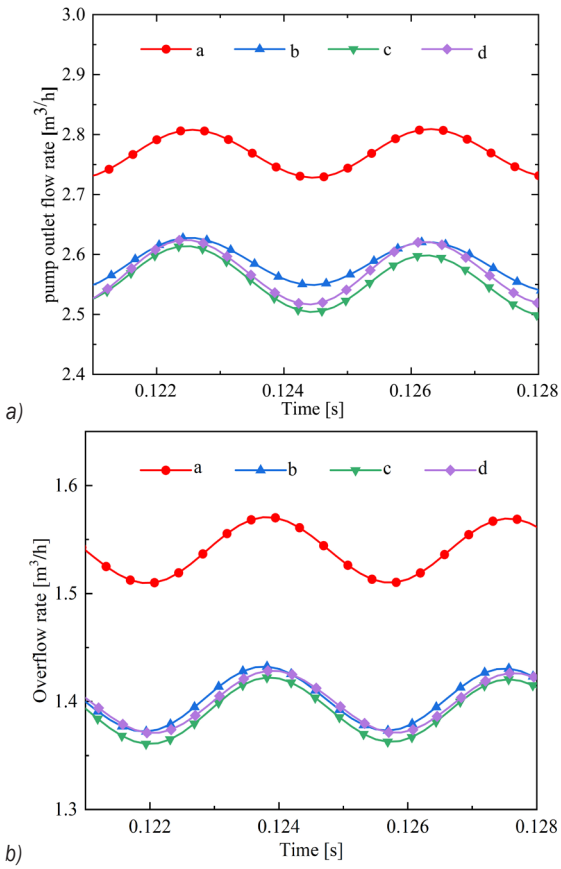

Fig. 7. *Comparison of outlet flow rates; a) pump outlet flow rate, and b) overflow rate*

The valve template mesh module is used to process the corresponding fluid domain mesh. The motion surface, cylindrical surface, and termination end surface of the volume chamber are set, and the motion direction is *X*-axis. The minimum gap is 0.1 mm and the maximum stroke is 9 mm. Since the valve spool belongs to the moving parts, the valve template mesh module is also used for mesh division. Other parts such as connecting pipes and sliding oil pump inlet and outlet are meshed using the general mesher module.

The domain of computing fluids is meshed by using the pumplinx professional pump and valve model. The lubricating oil pump rotor is meshed using the rotor template mesh module. The size of the rotor mesh is adjusted to fine. There are traction and compressed volume chambers in the direction of movement of the valve spool valve. Consequently, the valve template mesh is used for grid processing, and the other parts are mesh using the general mesh module. The fluid domain grid for joint simulation calculation is shown in Fig. 6. After grid partition, each grid is connected by connect selected boundaries via moving grid interface (MGI) and grid interaction surface is added to form a complete grid connecting the fluid fields of the pump-valve joint simulation calculation.

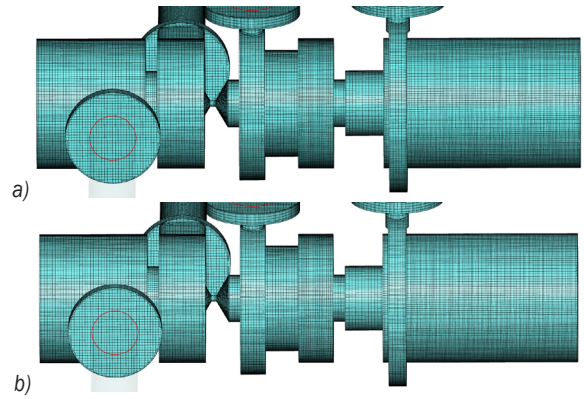

Fig. 8. *Grid division of a) pressure differential valve, and b) lubricating oil pump*

1.5 Initial and Boundary Conditions

4050 aviation lubricating oil is used as the fluid medium. Its service temperature is –40 °C to 200 °C, and it can withstand temperatures up to 220 °C for a short time. It has excellent high and low temperature use ability. The equation of density changing with temperature is:

$$\rho_t = \rho_{20} - \beta\left(t - 20\right), \tag{8}$$

where ρ_t, ρ_{20} are the density at temperature t 20 °C in [g/cm³]; the coefficient of β is different with different lubricating oil, β is 0.000035.

Lubricating oil kinematic viscosity and temperature calculation equation:

$$\ln\ln\left(v + A\right) = B - C\ln T, \tag{9}$$

where A, B, C are coefficients related to fuel. By looking up the relevant information, A = 0.6, B = 21.52, C = 3.54. The density of 4050 lubricating oil at 25 °C ρ = 0.972025 g/cm³, dynamic viscosity μ = 0.045844198 Pa·s.

The gerotor model, valve model, turbulence model, cavitation model, translation 1~DOF model

and flow model are added to the model window. First, select the reference pump in the extended model and set the speed to 2500 rpm and the rotation axis to the *Z* axis. In advanced mode, the translation 1~DOF module is set up, the specific parameters are shown in Table 4.

Table 4. *Translation 1~DOF model parameters*

Valve spool mass [kg]	Spring stiffness [N/m]	Spring preload [N]	Initial displacement [m]	Initial velocity [m/s]	Minimum gap [mm]	Maximum gap [mm]
0.05	4900	69.8	0	0	0.1	9.0

By comparing three turbulence models, namely Standard k–ε, renormalization group (RNG) k–ε, and realizable k–ε, it is found that the RNG $k-\varepsilon$ model has higher credibility and accuracy in analysing a wider range of flow characteristics compared to the Standard $k-\varepsilon$ model. The realizable $k-\varepsilon$ model performs well in predicting moderate-intensity swirling flow. Since this paper does not involve swirling flow issues, the RNG $k-\varepsilon$ turbulence model is ultimately chosen for numerical calculations.

Table 5. *Computational setup of pump model*

Boundary conditions	Boundary type
Location	
Inlet of model pump	Total Pressure(one-atmosphere)
Outlet of model pump	Total Pressure(one-atmosphere)
Physical wall surfaces	No-slip wall
Interfaces on both side of impeller	
Transient state	Transient rotor-stator

Table 6. *Computational setup of valve model*

Boundary conditions	Boundary type
Location	
Inlet of the middle cavity	Total Pressure(one-atmosphere)
outlet of the overflow cavity	Total Pressure(one-atmosphere)
Moving wall surfaces	Slip wall
Translation 1~DOF	Dynamic BC
Velocity	trans_1d.velocity, 0 m/s, 0 m/s
Remaining physical wall surfaces	No-slip wall
Control for transient simulation	
Time step	3.3×10^{-5} s
Total time	0.24 s
Convergence criterion	10^{-4}

During the work process, the internal and external rotors of the lubricating oil pump are constantly meshed and separated, and cavitation occurs during numerical calculations. The full cavitation model includes the N-S equation and the commonly used turbulence model. The phase change rate equation is obtained by improving the Rayleigh-Plesset bubble dynamics equation, so the full cavitation model is selected for calculation.

After the basic setting of the model is completed, the solution parameter settings of the lubricating oil pump and pressure differential valve are shown in Tables 5 and 6, respectively.

1.6 Parameters for the Calculation Schemes

This paper mainly studies the transient flow characteristics of the differential pressure valve with different valve spool damping orifice structures. By changing the diameter and length of the damping orifice, this paper designs five kinds of valve spools with different structures. When the structure of the damping orifice changes, its mass will also change. Fig. 10 shows the 3D structure of the valve spool. Table 7 shows the specific parameters of damping orifice under different structures.

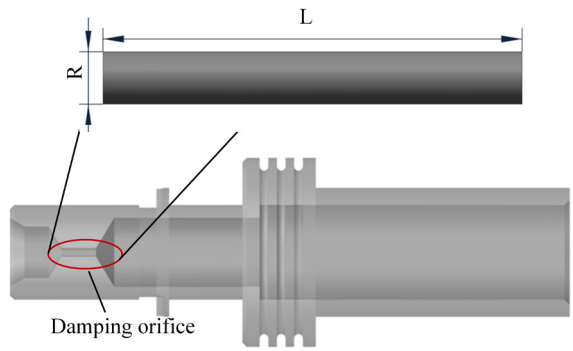

Fig. 9. *The 3D model with valve spool*

Table 7. *Specific parameter of damping orifice in different structures*

Scheme	Diameter [mm]	Length [mm]	Mass [g]
a	0.3	0.894	50.17
b	0.6	0.894	50.10
c	1.0	0.894	50.00
d	1.0	2.0	50.44
e	1.0	4.0	51.24

2 EXPERIMENTAL SETUP AND MEASUREMENT

Fig. 10 is the diagram of the transient flow characteristics test bench for pressure differential valve. The valve working system test bench includes oil tank, lubricating oil pump, servo motor, vortex flowmeter, pressure differential valve, pressure pulsation sensor, electric valve, and valve pipeline.

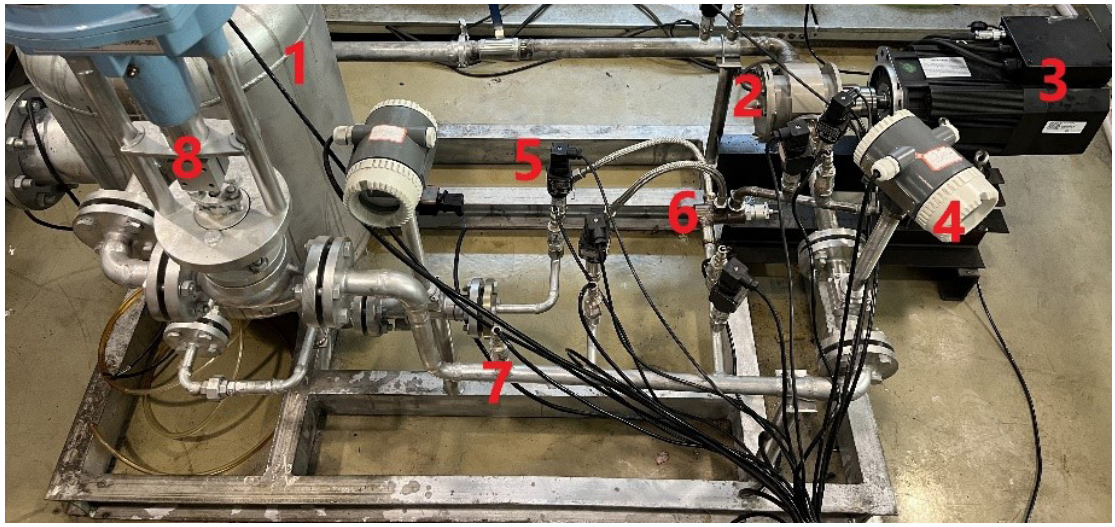

Fig. 10. *Pressure differential valve working system test bench; 1 oil tank, 2 lubricating oil pump, 3 servo motor, 4 vortex flowmeter, 5 temperature sensor, 6 pressure differential valve, 7 pressure pulsation sensor, 8 electric valve*

Table 8. *Main test equipment specifications*

Instrument	Model	Performance index
Pressure sensor	SCYG410 0 MPa to 0.5 MPa / 2.0 MPa	±0.1% FS
Turbine meter	LUGB-DN15/DN25	1.5 MPa to 1.6 MPa
Electric control valve	PHLZ-206S-30	1.6 MPa
Servo motor	VA-XX-4T5.5G	3.7 kw

The valve pipeline includes closed loop circuit, valve inlet pipeline, valve oil supply pipeline, valve overflow pipeline and valve intermediate bearing cavity inlet pipeline.

In this paper, 4050 aviation lubricating oil is used as the test medium. During the test, the ball valve is first opened, the servo motor is turned on to adjust the speed to 2500 rpm and the electric control valve is used to adjust the working pressure of the system between 0.3 MPa to 0.6 MPa. The data acquisition box is used to transfer the signal of the pressure sensor to the computer, and the pressure change is displayed in real time. The sampling frequency is 10240 Hz. Table 8 is the main test equipment and test component specifications of the test bench.

3 RESULT AND DISCUSSION

3.1 Experimental Test of Pressure Differential Valve

In this paper, pressure differential valve with damping orifice structure of Φ 1 mm × 0.894 mm is taken as an example (Method c in Table 7) for experimental verification. Figs. 11a and b respectively show the comparison of the inlet pressure pulsation and oil supply frequency spectra of pressure differential valve between the simulation results and the experimental results. It can be seen from the diagram that the main frequency of the inlet pressure pulsation and the oil supply pressure pulsation is within 5 % of the experimental value. Fig. 12 shows the comparison between the simulation and test results of pump outlet flow rate and valve overflow flowrate. It can be seen from the figure that the error between the simulation value and the test value is within 10 %. The comparison results show that the simulation model and simulation method have certain reliability.

3.2 Transient high-pressure lubricating oil flow behaviour in pressure differential valve

Taking pressure differential valve with damping orifice structure of Φ 1 mm × 0.894 mm as an example, the flow characteristics of transient high pressure lubricating oil inside the valve are studied. Fig. 13 shows the change of valve spool velocity and displacement with opening time. It can be seen that the valve spool begins to move at 0.02 s. With the increase of opening time, the valve spool displacement gradually increases. At 0.2 s, the valve

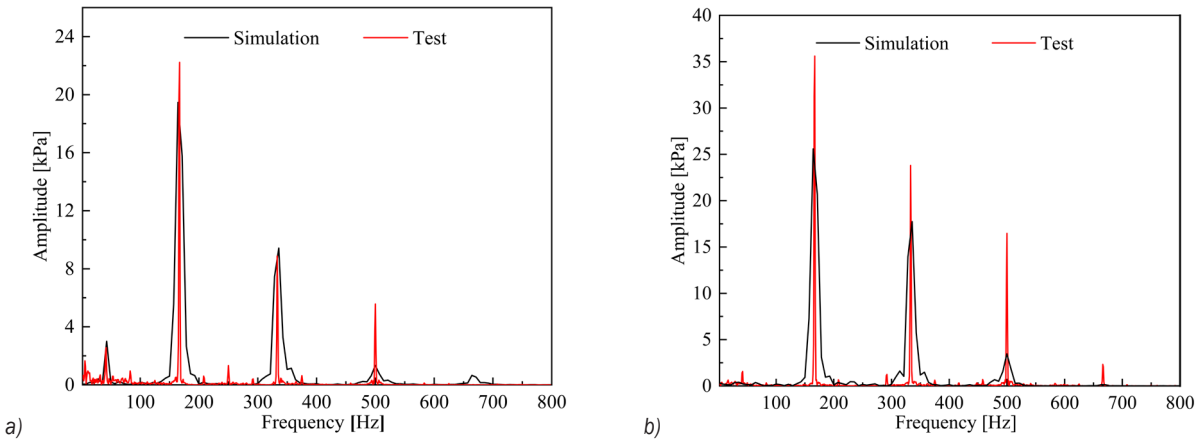

Fig. 11. *Comparison of pressure pulsation spectra; a) inlet valve pressure pulsation, and b) oil supply pressure pulsation*

spool displacement gradually stabilizes, and the displacement is 8.87 mm. At 0.02 s to 0.035 s, the velocity of the valve spool increases rapidly, reaches the maximum value of 0.236 m/s at 0.035 s, and then begins to decline to about 0 m/s.

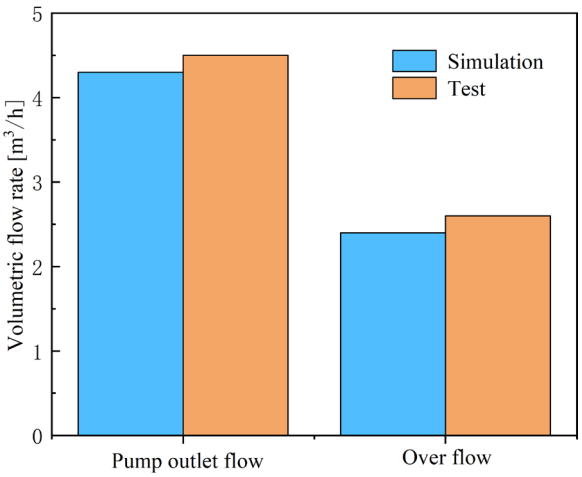

Fig. 12. *Comparison of outlet flow rate*

Fig. 14 shows the relationship between fluid force and spring force with valve spool displacement. The results show that the fluid force and spring force increase with the increase of valve spool displacement. In the range of 0 mm to 0.64 mm, the displacement of the valve spool is small, and the pressure increases rapidly due to the accumulation of lubricating oil at the entrance of the valve. The fluid force is greater than the spring force and the gap increases with the increase of the displacement. Then, as the displacement of the valve spool increases, the overflow orifice is opened, and the lubricating oil returns to the oil tank through the bypass pipeline and the overflow pipeline. In the whole opening process, the gap between the fluid force and the spring force is small, so the two play a leading role in the opening process of pressure differential valve.

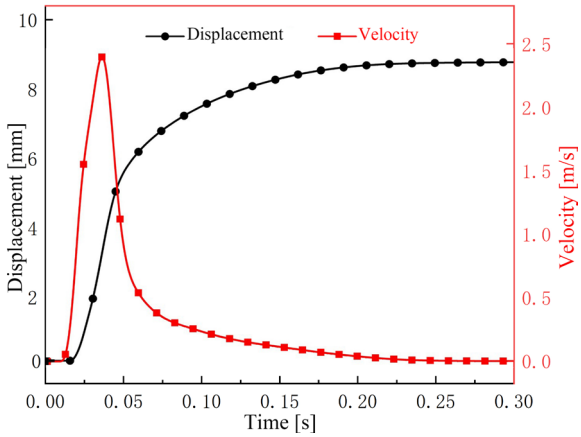

Fig. 13. *The relationship between both the valve spool displacement and velocity with the opening time*

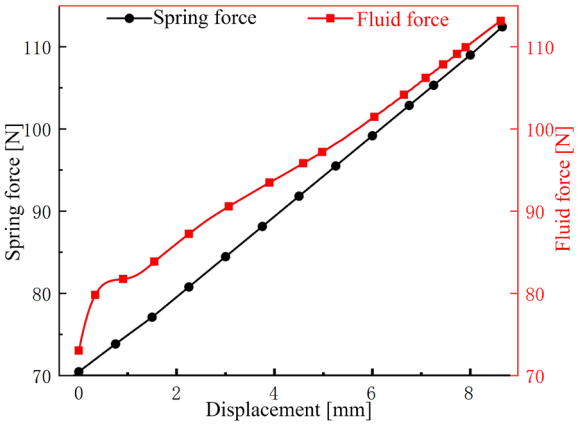

Fig. 14. *The fluid force and spring force performance with valve spool displacement*

Due to the limiting effect of the adjusting screw, the maximum displacement of the valve spool is 9 mm. It can be seen from Fig. 13 that during the opening process of pressure differential valve, the maximum displacement of the valve spool is less than 9 mm, and the movement velocity is very small when the valve spool reaches the maximum displacement, so the valve spool will not produce large kinetic energy to impact the adjustment screw to damage the valve component.

Fig. 15 shows the flow characteristics of high-pressure lubricating oil in pressure differential valve at 0.02 s, 0.035 s, 0.05 s and 0.065 s. Figs. 15a and b are the pressure and velocity contours of the central section of the valve, respectively. It can be found that during the opening process, the inlet pressure of the valve gradually increases, and the thrust acting on the gradually increasing head of the valve spool so that the valve spool begins to move. When the valve spool moves to the right and the overflow orifice is opened, the internal pressure of the valve finally reaches a stable state due to the overflow effect of the valve.

At 0.02 s, the oil supply pressure is about 349 kPa, the inlet pressure of the valve spool head is about 391 kPa. The valve spool head is subjected to a large thrust, and the valve spool begins to move. The maximum velocity projection in the X direction appears at the damping orifice, which is approximately 16.68 m/s. The high-pressure lubricating oil enters the inner chamber of the valve spool through the damping orifice. At this time, the volume chamber is not fully filled, the chamber pressure is about 92 kPa, and a large pressure gradient appears at the damping orifice.

At 0.035 s, the oil supply pressure is about 1219 kPa, and the inlet pressure of the valve spool head is about 1257 kPa, and the valve overflow orifice begins to be opened. At this time, the displacement of the valve spool increases rapidly, the volume of the inner chamber decreases rapidly, and the internal lubricating oil pressure reaches 3000 kPa. The maximum velocity projection in the X direction appears at the damping orifice at about -41.14 m/s, and the lubricating oil flows from the inner chamber to the valve inlet.

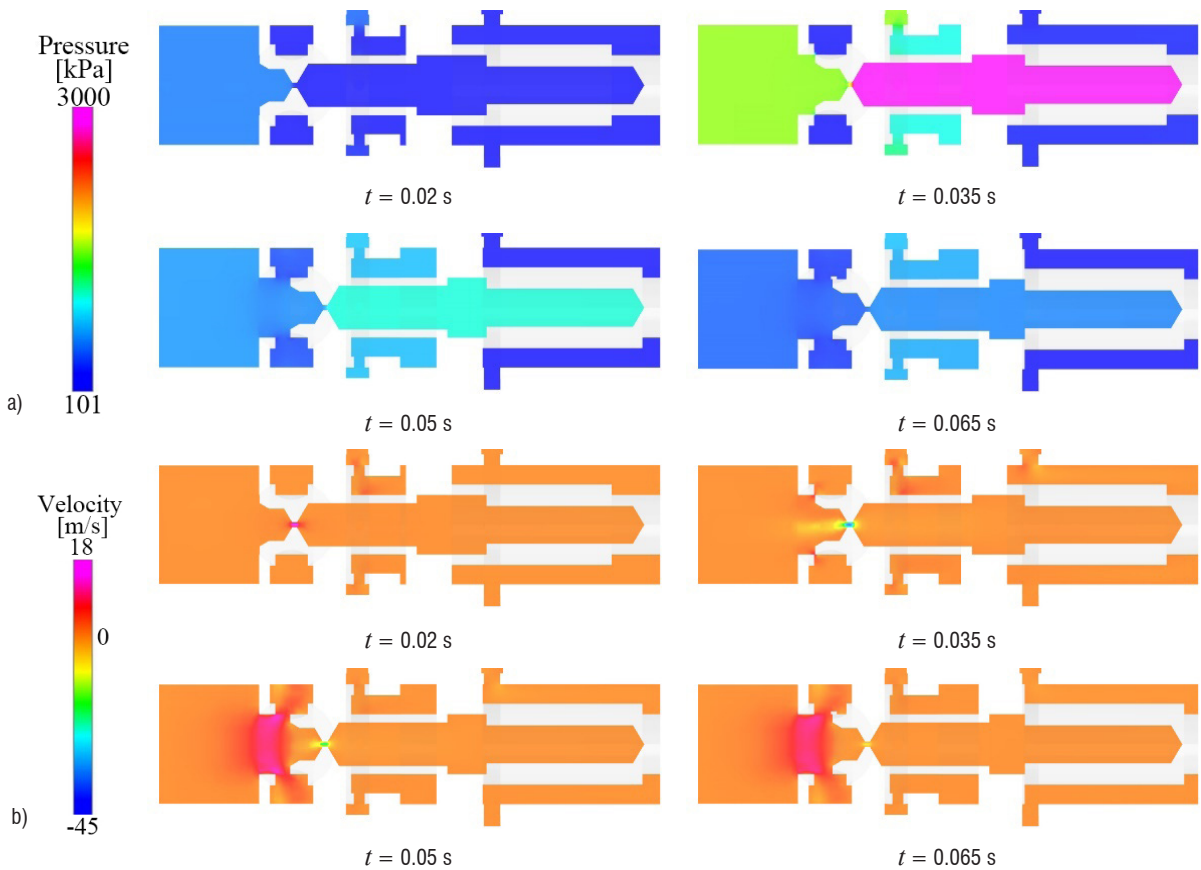

Fig. 15. *Pressure and velocity distributions in pressure differential valve at different moments: a) pressure distributions, and b) velocity distributions*

At 0.05 s, the movement velocity of the valve spool decreases, the movement displacement continues to increase, and the pressure drop characteristics of pressure differential valve increase with the increase of the valve opening. The oil supply pressure is reduced to 683 kPa, the inlet pressure of the valve spool head is 570 kPa, and the pressure in the inner chamber is about 1050 kPa. The maximum flow velocity projection in the X direction appears at the valve inlet area of about 12.05 m/s. The flow velocity of high-pressure lubricating oil at the damping orifice is reduced by about -23 m/s, and the valve opening is about 2.75 mm.

At 0.065 s, the pressure regulating characteristics of the valve begin to stabilize. With the slow increase of the valve spool displacement, the valve spool velocity decreases to 0.042 m/s. the valve opening continues to increase. The oil supply pressure is about 565 kPa, the inlet pressure of the valve spool head is about 460 kPa, and the pressure in the chamber of the valve spool gradually decreases to about 500 kPa. The pressure difference before and after the damping orifice is small, which makes the flow rate continue to decrease to about –0.9 m/s. The maximum velocity projection in the X direction appears in the valve inlet area about 12.05 m/s, and the valve opening is about 3.52 mm.

With the increase of opening time, the displacement and velocity of the valve spool are finally stabilized at about 8.87 mm and 0 m/s, respectively. The high-pressure difference before and after the valve spool damping orifice gradually disappears. The flow state of high-pressure lubricating oil inside the valve is relatively stable. The valve opening is maintained at about 5.8 mm, and the excess lubricating oil returns to the oil tank through the overflow pipeline and the bypass pipeline.

Fig. 16 shows the relationship between the valve inlet pressure and the oil supply pressure with the opening time. From the diagram, it can be seen that in the initial stage, the lubricating oil pump has not reached the specified speed, the oil supply quantity is less, and the valve oil supply pipeline is longer, so the valve inlet pressure is prior to the oil supply pressure response. At about 0.012 s, the oil supply pressure begins to rise. At 0.035 s, the two branch pressures of the valve reach the maximum value. After that, the overflow orifice begins to open with the increase of the displacement of the valve spool, and the valve opening gradually increases, which makes the two branch pressures gradually smaller. Finally, the oil supply pressure is stable at 521.7 kPa, and the valve inlet pressure is stable at 422.6 kPa.

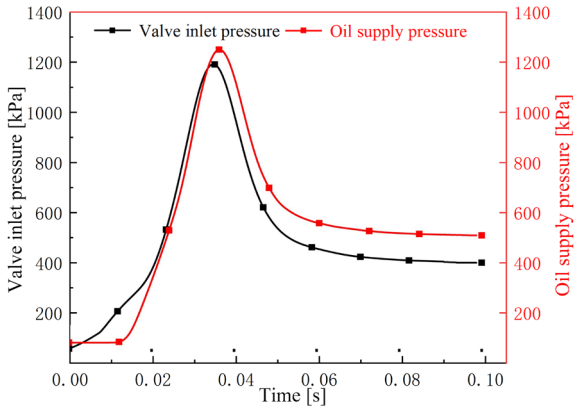

Fig. 16. *The relationship between both inlet pressure and oil supply pressure with the opening time*

3.3 Movement Performance of the Valve Spool with Different Damping Orifice Structures

Fig. 17 shows the relationship between valve spool displacement and opening time under different valve spool damping orifice structures. It can be seen that at 0.019 s, the valve spool structure of Φ 1 mm × 4 mm first begins to move, and at 0.02 s, the other four valve spool structures begin to move. As the diameter of the damping orifice gradually increases, the maximum motion displacement of the valve spool gradually increases, and the time required to reach a steady state gradually decreases. When the length of the damping orifice gradually increases, the influence on the maximum motion displacement of the valve spool is relatively small, but the time required to reach a steady state gradually increases. Under different valve spool structures, the first valve spool structure to reach a stable state is Φ 1 mm × 0.894 mm.

Fig. 18 shows the variation of valve spool velocity with displacement under different valve spool damping orifice structures. It can be seen that under different damping orifice structures of the valve spool, the shapes of the five velocity curves are relatively similar. At the beginning of the movement of the valve spool, the movement velocity of the valve spool rapidly increases and reaches its maximum value at a displacement of about 0.15 mm. Afterwards, it gradually decreases to around 0 m/s as the displacement increases. As the diameter or length of the damping orifice gradually increases, the maximum velocity of the valve spool gradually decreases. When the valve spool structures are respectively Φ 0.3 mm × 0.894 mm, Φ 0.6 mm × 0.894 mm, Φ 1 mm × 0.894 mm, Φ 1 mm × 2 mm and Φ 1 mm × 4 mm, the maximum motion velocity is 0.226 m/s, 0.209 m/s, 0.191 m/s, 0.183 m/s and 0.174 m/s, respectively. The

smaller the diameter or length of the damping orifice, the greater the maximum velocity of the valve spool.

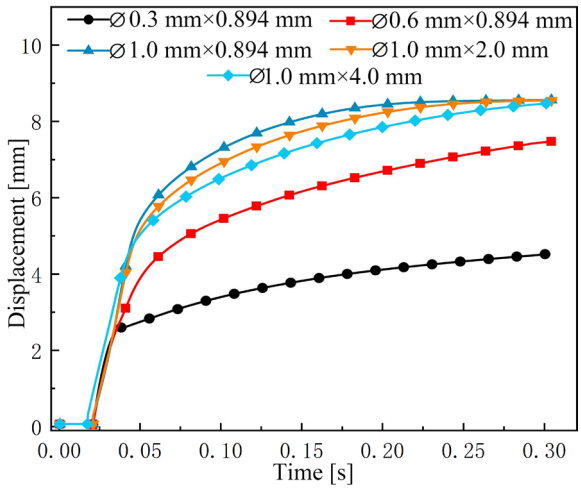

Fig. 17. *The relationship between the valve spool displacement and opening time for different damping orifice structures*

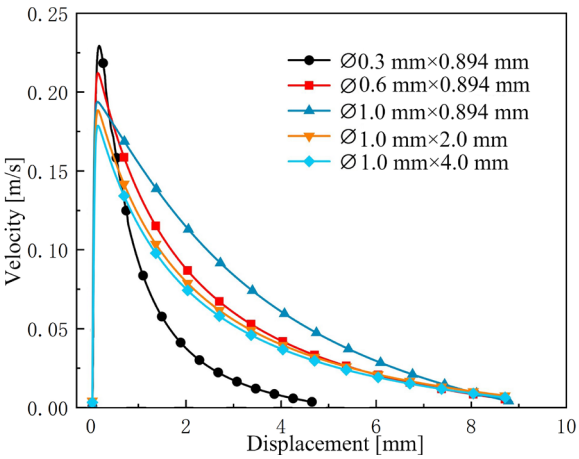

Fig. 18. *The relationship between the valve spool velocity and displacement for different damping orifice structures*

Fig. 19 shows the variation of fluid force with opening time under different valve spool damping orifice structures. Before 0.0087 s, due to the initial rotation of the lubricating oil pump, the system pressure is generally low, the valve inlet pressure and the oil supply pressure are relatively small, so the fluid force acting on the valve spool is almost zero. At 0.0087 s to 0.027 s, the valve spool is in the initial motion state, the motion displacement is very small, the overflow orifice has not been opened, and the diameter of the pipe outlet is small, which makes the pressure of the whole system increase, the lubricating oil gathers at the entrance of the valve, and the fluid force increases rapidly. The fluid force is 80.06 N at 0.027 s. After that, the fluid force continues to increase slowly and reaches a steady state at 0.275 s. As the diameter of the valve spool damping orifice increases, the fluid force gradually increases when it reaches a stable state. When the length of the valve spool damping orifice increases, the influence of the fluid force is very small. In the steady state, when the valve spool structures are respectively Φ 0.3 mm × 0.894 mm, Φ 0.6 mm × 0.894 mm, Φ 1 mm × 0.894 mm, Φ 1 mm × 2 mm and Φ 1 mm × 4 mm, the fluid force is 92.08 N, 106.91 N, 112.43 N, 112.34 N and 111.85 N, respectively.

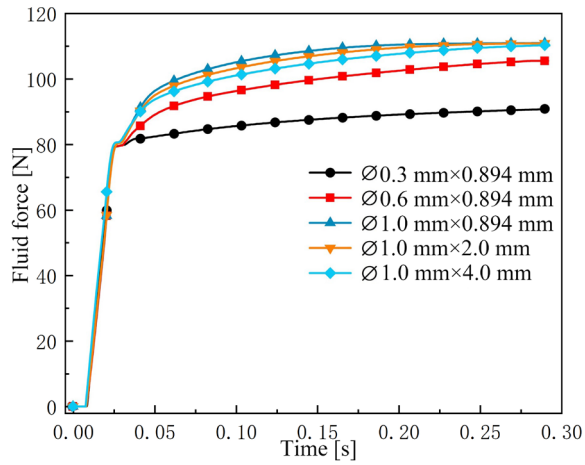

Fig. 19. *The relationship between the fluid force and opening time for different damping orifice structures*

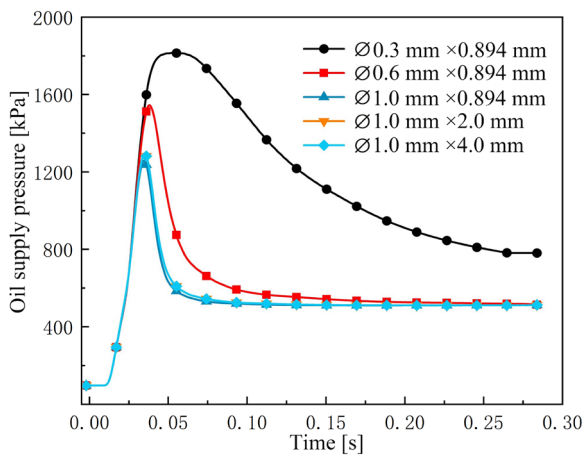

Fig. 20. *The relationship between the oil supply pressure and opening time for different damping orifice structures*

Fig. 20 shows the variation of oil supply pressure with opening time under different valve spool damping orifice structures. At the beginning, the lubricating oil has not yet entered the supply pipeline, and the change in supply pressure is minimal. At 0.02 s, the supply pressure begins to increase. As the

diameter of the valve spool damping orifice increases, the time required to reach the maximum oil supply pressure gradually decreases, and the maximum pressure also gradually decreases. When the length of the damping orifice in the valve spool increases, the impact on the oil supply pressure is minimal, and the pressure curve almost overlaps. When the damping orifice structures of the valve spool are respectively Φ 0.3 mm × 0.894 mm, Φ 0.6 mm × 0.894 mm, Φ 1 mm × 0.894 mm, Φ 1 mm × 2 mm and Φ 1 mm × 4 mm, the peak oil supply pressure is 1855 kPa, 1568 kPa, 1562 kPa, 1545 kPa and 1549 kPa, respectively. When the valve spool structure is Φ 0.3 mm × 0.894 mm, the peak pressure of the oil supply pressure is extremely high and the high-pressure state lasts longer, and the pressure drop is slower, which to some extent will affect the safe use of the valve.

In order to better understand the influence of different valve spool damping orifice structures on the opening process of pressure differential valve, Fig. 21 shows the pressure and velocity contours of the central section inside the valve when the oil supply

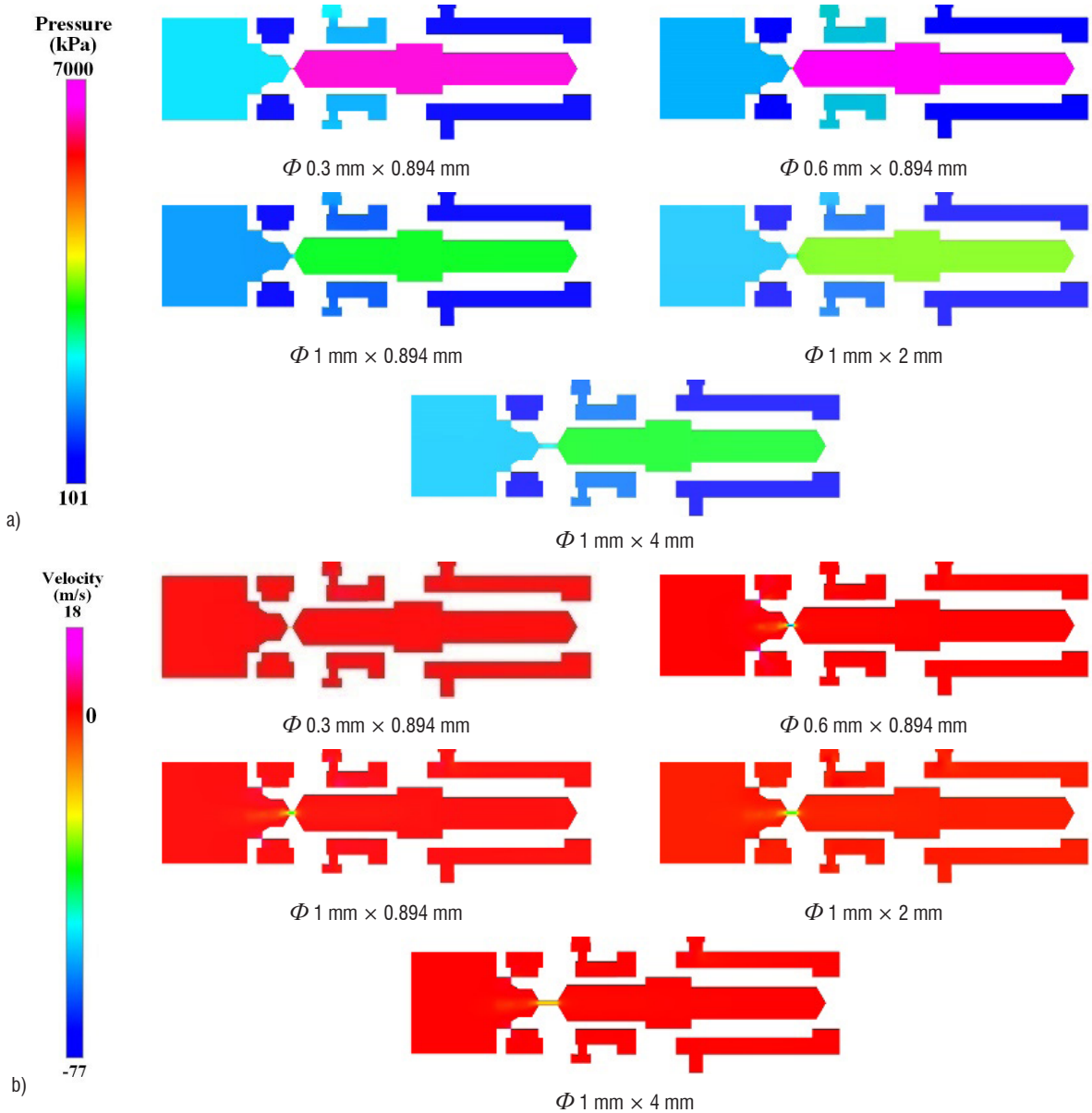

Fig. 21. *Pressure and velocity contours of the valve spool valve flow field when the oil supply pressure reaches the peak; a) static pressure contours for 5 damping orifice structures; and b) velocity contours for 5 damping orifice structures*

pressure reaches the maximum. It can be seen from Figs. 17 to 19 that when the valve spool displacement is 3 mm, the valve opening is in a critical state, and the overflow orifice is about to open. When it is greater than 3 mm, the valve opening increases gradually, the oil supply pressure decreases gradually, and the increase rate of fluid force decreases rapidly. As the displacement increases, the fluid force remains relatively stable. When the oil supply pressure reaches the maximum value, the damping orifice structures of the valve spool are respectively Φ 0.3 mm × 0.894 mm, Φ 0.6 mm × 0.894 mm, Φ 1 mm × 0.894 mm, Φ 1 mm × 2 mm and Φ 1 mm × 4 mm, and the valve spool displacement is 3.02 mm, 3.11 mm, 3.15 mm, 3.22 mm, and 3.32 mm, respectively. The velocity of the valve spool is 0.01667 m/s, 0.05071 m/s, 0.07653 m/s, 0.04829 m/s and 0.04226 m/s, respectively. The fluid force is 83.91 N, 86.09 N, 86.24 N, 85.78 N and 86.58 N, respectively.

When the oil supply pressure reaches the peak value, the valve opening is relatively small, and the rapidly increasing fluid force causes the lubricating oil

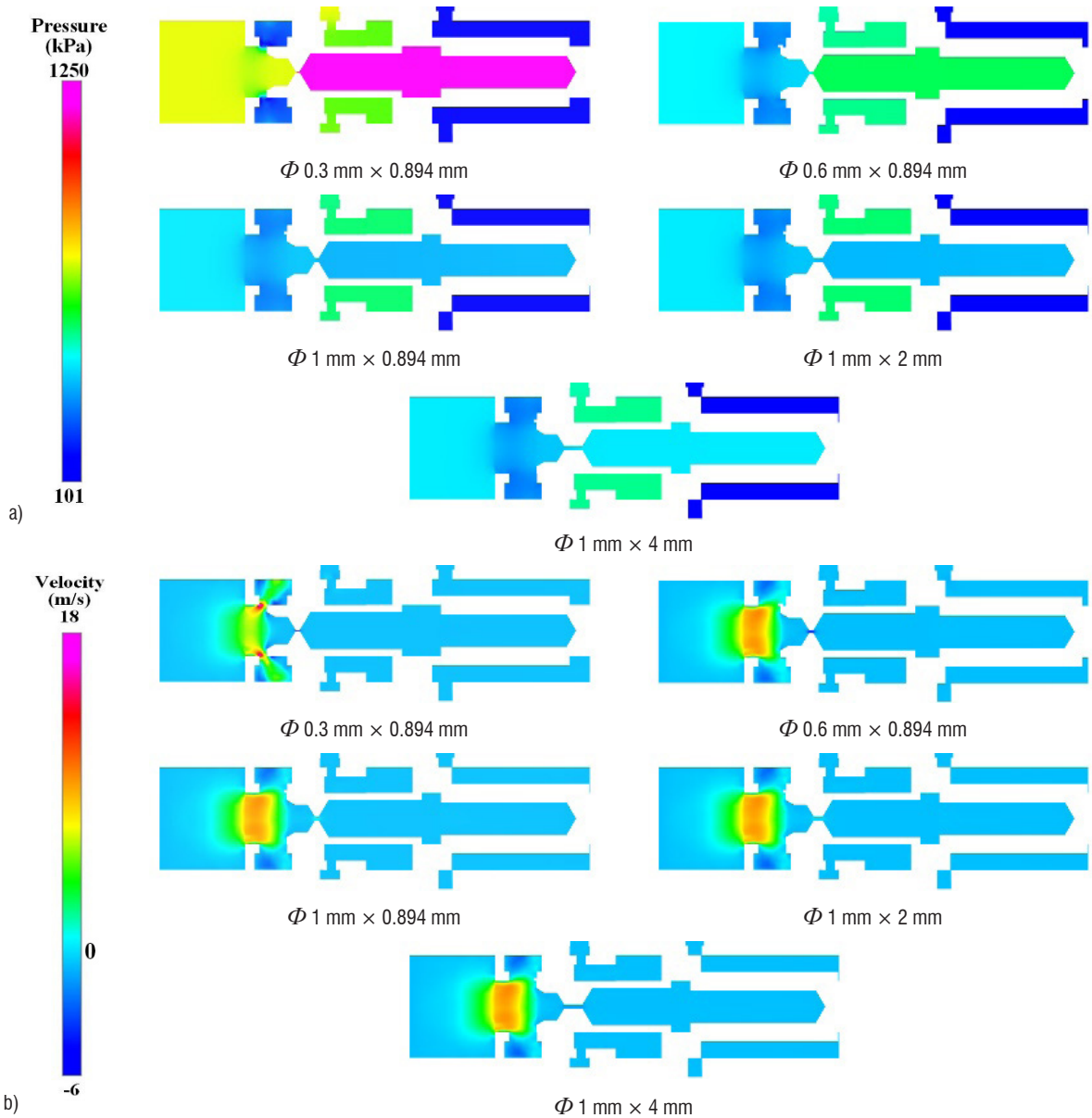

Fig. 22. *Pressure and velocity contours of the valve spool valve flow field when the oil supply pressure reaches stable; a) static pressure contours for 5 damping orifice structures, and b) velocity contours for 5 damping orifice structureses*

in the inner chamber to be squeezed, and the pressure increases rapidly. As shown in Fig. 21, with the increase of the diameter of the damping orifice, when the structure of the valve spool damping orifice is *Φ* 0.6 mm × 0.894 mm, the internal chamber pressure reaches the highest due to the relatively high inlet pressure and oil supply pressure of the valve. At the same time, the pressure gradient reaches the highest before and after the damping orifice, and the flow velocity of the lubricating oil reaches the maximum, as shown in Fig. 21b, which is about –76.22 m/s. With the increase of the length of the damping orifice, the influence on the pressure and velocity contours of pressure differential valve is relatively small. The pressure in the inner chamber of the valve spool is basically about 3000 kPa, and the velocity gradient at the damping orifice is relatively small.

Fig. 22 shows the pressure and velocity contours of the central section of pressure differential valve when the oil supply pressure is stable. From Figs. 17, to 19, it can be seen that in the steady state, the damping orifice structure of the valve spool is *Φ* 0.3 mm × 0.894 mm, *Φ* 0.6 mm × 0.894 mm, *Φ* 1 mm × 0.894 mm, *Φ* 1 mm × 2 mm and *Φ* 1 mm × 4 mm, the valve spool displacement is 4.66 mm, 7.79 mm, 8.87 mm, 8.87 mm, and 8.86 mm, respectively. The velocity of the valve spool is basically fluctuating around 0 m/s. The fluid force is 92.08 N, 106.9 N, 112.43 N, 112.34 N and 111.85 N, respectively.

As shown in Fig. 22a, the oil supply pressure is stable at this time. When the valve spool structure is *Φ* 0.3 mm × 0.894 mm, the diameter is very small, the internal high-pressure lubricating oil flows to the valve inlet through the damping orifice, the resistance along the way is very large, and the decompression process is relatively slow. The pressure in the inner chamber of the valve spool is significantly higher than that of the other four structures. As the diameter of the damping orifice increases, the pressure in the chamber of the valve spool and the pressure gradient at the damping orifice gradually decrease. As shown in Fig. 22b, as the valve spool diameter increases, the valve opening gradually increases, the flow area of the overflow orifice increases, and the velocity gradient of the high-pressure lubricating oil at the valve spool inlet decreases. With the increase of the length of the valve spool damping orifice, the influence on the pressure and velocity contours of pressure differential valve is very small.

4 CONCLUSIONS

In this paper, a transient high pressure lubricating oil flow model of pressure differential valve is established. Through the joint simulation of the two-stage internal gear pump and pressure differential valve, the flow characteristics of the high-pressure lubricating oil in the valve during the opening of pressure differential valve are analysed. In addition, the influence of the structure of the valve spool damping orifice on the pressure regulation characteristics of pressure differential valve is also compared and analysed.

The following conclusions can be made. The opening time of the differential pressure valve in the lubricating oil supply subsystem is very fast, and the time for the valve spool to reach the maximum stroke is less than 0.3 s. During the valve opening process, the valve inlet pressure and the oil supply pressure increase rapidly with time. The larger pressure makes the valve spool begin to move, the overflow orifice gradually opens, the pressure regulation of the valve is gradually significant, and the inlet pressure and oil supply pressure of the valve gradually decrease and reach stability. The fluid force increases rapidly at first, and the growth rate of the fluid force is obviously reduced due to the overflow effect, and finally reaches a stable state. The difference between the spring force and the fluid force is relatively small. During the valve opening process, the two together affect the pressure regulation characteristics of pressure differential valve. The velocity of the valve spool increases rapidly with the increase of displacement at the beginning, and then decreases gradually due to the overflow effect. When the displacement of the valve spool reaches stability, the velocity fluctuates around 0 m/s.

The pressure regulation characteristics of pressure differential valve during opening process are quantified. When the inlet pressure and outlet pressure are both 101 kPa, the minimum fluid force of the valve spool is 92.08 N, the maximum velocity is 0.226 m/s, the maximum oil supply pressure is 1855 kPa, and the maximum oil supply pressure is 800 kPa when it reaches a steady state. When the damping orifice structure of the valve spool is *Φ* 0.3 mm × 0.894 mm, the pressure regulation performance is poor, and the oil supply pressure reaches the maximum value for a long time and the pressure drops slowly, which has a great influence on the lubrication function of the lubrication system, and even causes damage to other components such as the engine.

The influence of valve spool damping orifice structure on the transient flow characteristics and

valve spool motion characteristics during the opening process of pressure differential valve. When the diameter of the damping orifice increases from 0.3 mm to 1.0 mm, the maximum displacement of the valve spool increases from 4.66 mm to 8.87 mm, the maximum velocity of the valve spool decreases from 0.226 m/s to 0.191 m/s, and the maximum oil supply pressure decreases from 1855 kPa to 1288 kPa. When the valve spool displacement reaches the maximum, the fluid force increases from 83.91 N to 86.24 N, and the oil supply pressure decreases from 800 kPa to 521 kPa. When the length of the valve spool damping orifice increases from 0.894 mm to 4.0 mm, the maximum displacement of the valve spool is about 8.85mm, the maximum velocity of the valve spool decreases from 0.191 m/s to 0.174 m/s, and the maximum oil supply pressure is about 1500 kPa. When the displacement of the valve spool valve reaches the maximum, the fluid force is about 112 N, and the oil supply pressure is about 521 kPa.

The internal and external mechanisms are as follows. The damping orifice structure of pressure differential valve has little effect on the start time of the valve spool. With the increase of the diameter of the damping orifice, the resistance of the valve spool throat decreases, and the pressure gradient between the inner cavity and the valve core head decreases. The high-pressure lubricating oil in the chamber is easier to flow back to the head of the valve spool through the damping orifice, and the high pressure in the inner chamber drops faster, and the maximum displacement of the valve spool also increases. At the same time, the fluid force during the movement of the valve spool also increases, and the moving velocity of the valve spool decreases. The increase of the displacement means that the opening of the valve gradually increases, and the pressure reduction characteristics of pressure differential valve gradually become obvious. The large flow area of the overflow orifice enables the high-pressure lubricating oil to quickly return to the tank through the overflow pipeline and the bypass pipeline. The inlet pressure and oil supply pressure of the valve decrease rapidly, and the oil supply pressure is more in line with the allowable requirements of the lubricating oil system. When the length of the damping orifice increases, it has little effect on the pressure regulation characteristics of pressure differential valve and the motion state of the valve spool.

5 REFERENCES

[1] Li, A., Zhang, S., Shi, H., Zhang, W.L. (2012). Simulation study for lubrication oil supply system for an aero-engine. *Journal of Shenyang Aerospace University*, vol. 29, p. 21-24, **DOI:10.3969/j.issn.2095-1248.2012.03.005**. (in Chinese)

[2] Li, Q. H., Zhang, J. (1991). *Aeroengine Reliability Engineer Qualification Training Course Textbook: Chapter 12 Aeroengine Condition Monitoring and Fault Diagnosis*. Beijing University of Aeronautics and Astronautics, Beijing.(in Chinese)

[3] Dumachenko, H.T., Kravitz, A.C. (1978). *Gas Turbine Engine*. National Defense Industry Press, Moscow (in Russian).

[4] Li, Y. (2010). *The Fault Diagnosis Analysis on a Model of the Air Engine Lubrication System*, PhD Thesis, Wuhan University of Technology, Wuhan. (in Chinese)

[5] Aeroengine Design Manual Editorial Board (2002). *Aeroengine Design Manual, Volume 12: Transmission and Lubrication Systems*. Aerospace Industry Press, Beijing. (in Chinese)

[6] Li, G.Q. (2011). Present and future aeroengine oil system. *Aeroengine*, vol. 37, no. 6, p. 49-52. (in Chinese)

[7] Wei, X.D. (2019). The present situation and future development of aero-engine lubricating oil system are analyzed. *Internal Combustion Engines and Accessories*, vol. 12, p. 63-64. (in Chinese)

[8] Li, G.Q. (2008). Analysis of altitude performance of aeroengine oil pump. *Aeroengine*, vol. 34, p. 46-47.

[9] Lai, Z.N., Karney, B., Yang, S., Wu, D., Zhang, F.X. (2017). Transient performance of a dual disc check valve during the opening period. *Annals of Nuclear Energy*, vol. 101, p. 15-22, **DOI:10.1016/j.anucene.2016.10.010**.

[10] Afshari, H.H., Zanj, A., Novinzadeh, A.B. (2010). Dynamic analysis of a nonlinear pressure regulator using bondgraph simulation technique. *Simulation Modelling Practice and Theory*, vol. 18, no. 2, p. 240-252, **DOI:10.1016/j.simpat.2009.11.001**.

[11] Cui, B.L., Lin, Z., Zhu, Z.C., Wang, H.J., Ma, G.F. (2017). Influence of opening and closing process of ball valve on external performance and internal flow characteristics. *Experimental Thermal and Fluid Science*, vol. 80, p. 193-202, **DOI:10.1016/j.expthermflusci.2016.08.022**.

[12] Sibilla, S., Gallati, M. (2008). Hydrodynamic characterization of a nozzle check valve by numerical simulation. *ASME Journal of Fluids Engineering*, vol. 130, no. 12, p. 1211011-12110112, **DOI:10.1115/1.3001065**.

[13] Beune, A., Kuerten, J.G.M., van Heumen, M.P.C. (2012). CFD analysis with fluid-structure interaction of opening high-pressure safety valves. *Computers & Fluids*, vol. 64, p. 108-116, **DOI:10.1016/j.compfluid.2012.05.010**.

[14] Chattopadhyay, H., Kundu, A., Saha, B.K., Gangopadhyay, T. (2012). Analysis of flow structure inside a spool type pressure regulating valve. *Energy Conversion and Management*, vol. 53, no. 1, p. 196-204, **DOI:10.1016/j.enconman.2011.08.021**.

[15] Han, Y., Zhou, L., Bai, L., Xue, P., Lv, W.N., Shi, W.D., Huang, G.Y. (2022). Transient simulation and experiment validation on the opening and closing process of a ball valve. *Nuclear Engineering and Technology*, vol. 54, no. 5, p. 1674-1685, **DOI:10.1016/j.net.2021.10.035**.

[16] Saha, B.K., Chattopadhyay, H., Mandal, P.B., Gangopadhyay, T. (2014). Dynamic simulation of a pressure regulating and shut-off valve. *Computers & Fluids*, vol. 101, p. 233-240, **DOI:10.1016/j.compfluid.2014.06.011**.

[17] Ray, A. (1978). Dynamic modeling and simulation of a relief valve. *Simulation*, vol. 31, no. 5, p. 167-172, **DOI:10.1177/003754977803100504**.

[18] Dasgupta, K., Karmakar, R. (2002). Dynamic analysis of pilot operated pressure relief valve. *Simulation Modelling Practice and Theory*, vol. 10, no. 1-2, p. 35-49, **DOI:10.1016/S1569-190X(02)00061-8**.

[19] Zhang, Z.H., Jia, L., Yang, L.X. (2019). Numerical simulation study on the opening process of the atmospheric relief valve. *Nuclear Engineering and Design*, vol. 351, p. 106-115, **DOI:10.1016/j.nucengdes.2019.05.034**.

[20] Sun, X.M., Qin, B.K., Bo, H.L., Xu, X.X. (2017). Transient flow analysis of integrated valve opening process. *Nuclear Engineering and Design*, vol. 313, p. 296-305, **DOI:10.1016/j.nucengdes.2016.12.014**.

[21] Yang, L., Wang, Z.J., Dempster, W., Yu, X.H., Tu, S.-T. (2017). Experiments and transient simulation on spring-loaded pressure relief valve under high temperature and high pressure steam conditions. *Journal of Loss Prevention in the Process Industries*, vol. 45, p. 133-146, **DOI:10.1016/j.jlp.2016.11.019**.

[22] Abdallah, H.K., Peng, J.H., Li, S.J. (2023). Analysis of pressure oscillation and structural parameters on the performance of deflector jet servo valve. *Alexandria Engineering Journal*, 63, p. 675-692, **DOI:10.1016/j.aej.2022.11.021**.

[23] Zang, J.-L., Yao, H.-Y., Zhang, F.-H., Liu, Z.-Y., Meng, J., Zhu, J.-M., Wang, Z.-M., Qian, J.-Y. (2022). Dynamic characteristics analysis of pilot valves with different inlet diameters installed on the main steam valve set. *Case Studies in Thermal Engineering*, vol. 34, art. ID 102004, **DOI:10.1016/j.csite.2022.102004**.

[24] Liu, J.-R., Jin, B., Xie, Y.-J., Chen, Y.,Weng, Z. T. (2009). Research on the electro-hydraulic variable valve actuation system based on a three-way proportional reducing valve. *International Journal of Automotive Technology*, vol. 10, p. 27-36, **DOI:10.1007/s12239-009-0004-6**.

[25] Simic, M., Herakovic, N. (2015). Reduction of the flow forces in a small hydraulic seat valve as alternative approach to improve the valve characteristics. *Energy Conversion and Management*, vol. 89, p. 708-718, **DOI:10.1016/j.enconman.2014.10.037**.

[26] Liu, J.L., Li, R.C., Ding, X.K., Liu, Q. (2022). Flow force research and structure improvement of cartridge valve core based on CFD method. *Heliyon*, vol. 8, no. 11, art. ID e11700, **DOI:10.1016/j.heliyon.2022.e11700**.

[27] Ye, J.J., Cui, J.X., Hua, Z.L., Xie, J.L., Peng, W.Z., Wang, W. (2023). Study on the high-pressure hydrogen gas flow characteristics of the needle valve with different spool shapes. *International Journal of Hydrogen Energy*, vol. 48, no. 30, p. 11370-11381, **DOI:10.1016/j.ijhydene.2022.04.073**.

[28] Ye, J.J., Zhao, Z.H., Cui, J.X., Hua, Z.L., Peng, W.Z., Jiang, P.C. (2022). Transient flow behaviors of the check valve with different spool-head angle in high-pressure hydrogen storage systems. *Journal of Energy Storage*, vol. 46, art. ID 103761, **DOI:10.1016/j.est.2021.103761**.

[29] Yang, X., Li, S.Z., Yang, B.B., Feng, Y.B. (2018). Influence of valve core and seat structure of overflow valve on flow field performance and optimization design. *Earth and Environmental Science*, vol. 170, art. ID 0221122, **DOI:10.1088/1755-1315/170/2/022112**.

[30] Han, M., Liu, Y., Liao, Y., Wang, S. (2021). Investigation on the modeling and dynamic characteristics of a novel hydraulic proportional valve driven by a voice coil motor. *Strojniški vestnik – Journal of Mechanical Engineering*, vol. 67, no. 5, p. 223-234, **DOI:10.5545/sv-jme.2021.7089**.

[31] Karanović, V., Jocanović, M., Baloš, S., Knežević, D., Mačužić, I. (2019). Impact of contaminated fluid on the working performances of hydraulic directional control valves. *Strojniški vestnik – Journal of Mechanical Engineering*, vol. 65, no. 3, p. 139-147, **DOI:10.5545/sv-jme.2018.5856**.